Evaluating the Performance of Gadobutrol and Gadoterate Meglumine for Contrast-Enhanced Magnetic Resonance Angiography of the thoracic aorta at 1.5T

Ashitha Pathrose (ashitha.pathrose@northwestern.edu)
Northwestern University Feinberg School of Medicine

Alyssa Singer
Northwestern University Feinberg School of Medicine

John Wence Cerne
Northwestern University Feinberg School of Medicine

Ali Serhal
Northwestern University Feinberg School of Medicine

Pascale Aouad
Northwestern University Feinberg School of Medicine

Julie Blaisdell
Northwestern University Feinberg School of Medicine

Ryan Avery
Northwestern University Feinberg School of Medicine

Michael Markl
Northwestern University Feinberg School of Medicine

Bradley Allen
Northwestern University Feinberg School of Medicine

James C. Carr
Northwestern University Feinberg School of Medicine

Research Article

Keywords: gadobutrol, gadoterate meglumine, Magnetic Resonance Angiography, contrast media, gadolinium

Posted Date: April 15th, 2022

DOI: https://doi.org/10.21203/rs.3.rs-1547836/v1

Abstract

PURPOSE

The purpose of this study was to systematically compare the intra-individual image quality, signal parameters, and aortic dimensions between equal doses of gadobutrol (GB) and gadoterate meglumine (GM) in patients undergoing contrast-enhanced MRA of the thoracic aorta.

METHODS

33 patients (50 ± 12 years, 30M) with aortic disease who underwent GB-enhanced thoracic aortic MRA were prospectively recruited to undergo a GM-enhanced MRA within 8 weeks. MRAs were obtained after administration of 0.2mL/kg of 1.0M GB and 0.4mL/kg of 0.5M GM at flow rate of 2mL/s. Aortic luminal signal intensities (SI) and contrast ratios (CR) with respect to trapezius were measured at three regions. Aortic orthogonal diameters were measured at six regions. Overall image quality, vessel wall conspicuity, and artifacts were scored by two radiologists.

RESULTS

GB demonstrated significantly higher SI at all regions when compared to GM (AAo: 234 ± 97 vs. 116 ± 29, $p < 0.001$; Arch: 206 ± 92 vs. 99 ± 24, $p < 0.001$; DAo: 265 ± 132 vs. 102 ± 28, $p < 0.001$). CR at all regions (AAo: 3.0 ± 1.1 vs. 2.7 ± 1.0, $p = 0.503$; Arch: 2.7 ± 1.0 vs. 2.8 ± 1.1, $p = 0.599$; DAo: 3.3 ± 1.5 vs. 3.0 ± 1.1, $p = 0.099$) and aortic diameters at all regions did not show any significant difference between GB and GM. Overall image quality, vessel wall conspicuity, and artifact scores did not significantly differ between GB and GM.

CONCLUSION

This intra-individual study found that for contrast-enhanced MRA of the thoracic aorta, CR, aortic diameter measurements, overall image quality, vessel wall conspicuity, and artifact scores were comparable between equal doses of GB and GM. However, GB showed significantly higher aortic luminal SI when compared to GM.

Introduction

Three-dimensional contrast-enhanced magnetic resonance angiography (CE-MRA) is routinely used for the assessment of a wide range of congenital and acquired diseases of the thoracic aorta (1–5). In the majority of cases, CE-MRA is optimally performed as a breath-hold, ECG-triggered first-pass MRA (FP-MRA) after intravascular injection of gadolinium-based contrast agents (GBCA) (6, 7). CE-MRAs have a higher contrast-to-background ratio when compared to non-contrast MRAs allowing for higher quality 3D

reconstructions. However, for effective CE-MRA of the thoracic aorta, imaging should be performed during peak contrast enhancement of aorta when the overlapping structures and background tissue are not enhanced. Several factors including the timing of the acquisition determined by the MRA protocol and vascular bolus geometry (i.e., the bolus width and peak height) determined by the GBCA formulation (8), contrast protocol, patient-specific parameters (e.g., cardiac function) (9), plays a major role in the intraluminal contrast enhancement with GBCAs.

The GBCA used for CE-MRA can be broadly classified into linear or macrocyclic agents according to their chemical structure, with macrocyclic GBCAs showing a more favorable safety profile and higher complex stability (10, 11). Of the available macrocyclic GBCAs, gadobutrol and gadoterate meglumine are the most widely used in the US. Previous studies have shown that these two agents differ in their ability to shorten T1 relaxation times, with non-ionic gadobutrol having a higher T1 relaxivity (1.5 times) when compared to ionic gadoterate meglumine (12). In addition, gadobutrol is administered at half the volume of gadoterate meglumine, even while they have the same amount of gadolinium, due to differences in formulation (gadobutrol is formulated at a concentration of 1 mmol/mL while gadoterate meglumine at 0.5 mmol/mL). Despite these differences in relaxivity and in formulated drug concentration, previous studies on CE-MRA for various vascular regions have failed to conclusively demonstrate differences in diagnostic performance of one agent over the other (13–20). Therefore, the purpose of this study was to systematically compare the intra-individual qualitative image quality as well as quantitative aortic dimensions and signal parameters between equal doses of gadobutrol and gadoterate meglumine for static 3D CE-MRA in patients with thoracic aortic disease.

Materials And Methods

Study Population

This single center, blinded, prospective, intra-individual comparison study was approved by the institutional review board and written informed consent was obtained from all study subjects. A total of 33 adult patients (mean age: 50 ± 12 years, range: 27–66 years, 30 males) who underwent a standard-of-care gadobutrol-enhanced clinical MRA of the thoracic aorta between 01/04/2017 and 09/01/2019 were recruited. Patients were excluded from research participation for the following reasons: known allergy to GBCA, history of acute or chronic kidney disease, history of kidney or liver transplant within 8 weeks of their clinical MRA, pregnant or breastfeeding women, any implanted device contraindicated for MRI, and claustrophobia. Subjects who developed any adverse effects during or after the clinical MRA (e.g., allergic reaction to GBCA) were also excluded. The recruited patients underwent a second gadoterate meglumine-enhanced research MRA within eight weeks after their clinical exam (average interval between the scans: 4.67 ± 1.99 weeks). All subjects had a glomerular filtration rate ≥ 60 mL/min/1.73m^2, as measured within 24 hours of the clinical as well as research MRA. Clinical indications for the thoracic aorta CE-MRA exam included patients with bicuspid aortic valve undergoing follow-ups, thoracic aortic aneurysms, aortic

insufficiency, Marfan syndrome, and non-rheumatic mitral valve prolapse. Demographic information is provided in detail in Table 1.

Table 1
Patient characteristics and indication for CMR

Age (years)		**50 ± 12**
Male (%)		30 (91%)
Reason for CMR referral (%)	BAV	17 (52%)
	Thoracic aortic aneurysm	7 (21%)
	BAV with thoracic aortic aneurysm	3 (9%)
	Dilated thoracic aorta	3 (9%)
	Aortic insufficiency	1 (3%)
	Marfan syndrome	1 (3%)
	Nonrheumatic mitral valve prolapse	1 (3%)

Data are shown as mean ± SD for age and number (%) for the categorical variables. BAV; Bicuspid Aortic valve, CMR; Cardiac Magnetic resonance imaging.

Magnetic Resonance Imaging protocol

All MRI examinations were performed on 1.5 Tesla whole-body MR systems (MAGNETOM Avanto/Aera/Espree, Siemens Healthcare). A six-element body matrix and a six-element spine matrix coil were used for signal reception and the body coil for transmission.

The MRA protocol consisted of localizer acquisitions in axial, coronal, and sagittal orientation, followed by a standard 3D MRA of the thoracic aorta using a breath-hold ECG gated 3D Gradient Recalled Echo (GRE) pulse sequences. At first, an unenhanced mask was acquired for the final subtraction to eliminate background signals. This was followed by the GBCA injection and CE-MRA acquisition in a sagittal-oblique plane. The imaging parameters were as follows: repetition time, 2.73ms; echo time, 1.01ms; flip angle, 40°; spatial resolution, 1.0×1.0×1.5mm^3, field-of-view, 400 x 400mm^2; slice thickness, 1.5mm (no interpolation); voxel size 1.0 × 1.0 × 1.5 mm^3; bandwidth, 590 Hz/Px; parallel imaging using GeneRalized Autocalibrating Partial Parallel Acquisition (GRAPPA) with acceleration factor, R = 3. All subjects underwent a comprehensive cardiac functional assessment during their standard-of-care clinical scan including balanced steady-state free-precession (bSSFP) cardiac cine and/or 2D and/or 3D phase-contrast flow imaging.

Contrast protocol

Following the unenhanced MRA acquisition, a test bolus of contrast agent (amount: 2 mL; flow rate: 2.0 mL/s), followed by a saline flush (20 mL; 2.0 mL/s), was given using an automatic infusion pump

(Spectris Solaris, Medrad, Bayer) to define the optimal acquisition time. The CE-MRA was obtained after intravenous administration of 0.2 mmol/kg body weight contrast media (amount: 10–28 mL for gadobutrol and 20–54 mL for gadoterate meglumine; flow rate: 2.0 mL/s) followed by a saline flush (20 mL; 2.0 mL/s). A double dose of GBCA is the clinical standard for comprehensive cardiac examination (of which the GB-enhanced MRA was part of) at our institution. We matched the dose for the research GM-enhanced MRA. For the clinical CE-MRA, 0.2 mL/kg of 1.0 M gadobutrol was used (Gadovist, Bayer AG). For the research CE-MRA, 0.4 mL/kg of 0.5 M gadoterate meglumine was used (Dotarem, Guerbet).

Image Analysis

Quantitative Analysis

The source images of the CE-MRA were used for quantitative evaluation of the two GBCA. Quantitative assessments were performed using a commercial software (Vitrea; Vital Images Inc.) by one observer (XX) with 1 year of experience in cardiovascular MRI. The observer was blinded to the type of GBCA and the patient's clinical and imaging history. The analysis was performed in a random order. Clinical and research MRA images from eleven subjects (1/3rd of our subjects; 22 studies) were evaluated by a second observer (XX) with 3 years of experience in cardiovascular imaging to evaluate interobserver reliability of quantitative analysis.

Signal intensity calculations: Aortic luminal signal intensity (SI) measurements were obtained by manually drawing circular regions of interest (ROIs) at the following aortic regions: mid-ascending aorta (MAAo) at the level of the pulmonary artery bifurcation, aortic arch (AArch) between the common carotid artery and the left subclavian artery, and descending aorta (DAo) mid-way between the left subclavian artery and the diaphragm. Additional ROIs were drawn at the trapezius muscle to calculate the lumen-to-muscle contrast ratios (CR) at each aortic region.

$$CR = \frac{SIatthelumen}{SIatthetrapeziusmuscle} \quad \text{Eq. 1}$$

Figure 1A shows the regions at which ROIs were drawn for SI and CR quantification.

Thoracic aortic orthogonal diameters

The diameter of the thoracic aorta was measured according to American Heart Association guidelines (7) at six levels as shown in the Fig. 1B. Three orthogonal measurements were taken at the sinus of Valsalva from sinus to sinus and two orthogonal diameter measurements were taken at the sinotubular junction (STJ), MAAo at the level of the pulmonary artery bifurcation), proximal AArch (at the level of the right brachiocephalic trunk), distal AArch (2 cm distal of the left subclavian artery) and middle DAo (middle between the left subclavian artery and the diaphragm). The diameters were measured after excluding the external wall (inner to inner). The maximum diameter measurement (instead of averaged measurements) at each orthogonal plane was compared between the two scans because many of our subjects were patients with significant aortic dilatation.

Qualitative analysis

Image quality analysis was performed independently by two radiologists (XX and XX) with 5 years of experience in cardiovascular imaging. The readers were blinded to the clinical symptoms, contrast agent used, and the results of other diagnostic procedures. The images were evaluated at the aortic root, MAAo, AArch, and the DAo for the following criteria: overall image quality, vessel wall conspicuity, and the presence of artifacts.

The images were scored for overall image quality using a 5-point Likert scale: 1 = very poor quality, non-diagnostic images; 2 = poor image quality, diagnosis suspected but not established, significant blurring and/or artifacts; 3 = fair image quality with diagnosis, moderate blurring and/or artifacts; 4 = good image quality, minimal blurring and/or artifacts; 5 = excellent image quality, sharply defined borders and no blurring or artifacts. Vessel wall conspicuity was scored using a 4-point Likert scale: 1 = non-diagnostic, vessel border unidentifiable; 2 = poorly seen, severe blurring of the vessel border; 3 = fairly seen, some vessel blurring; 4 = seen completely, good delineation of the vessel border. Artifacts (motion, susceptibility, aliasing) and their effect on confident evaluation of each segment were scored using a 4-point likert scale: 1 = severe artifact undermining confident evaluation; 2 = moderate artifact degrading confident evaluation; 3 = minimal artifact not interfering with evaluation; 4 = no artifacts. The qualitative scores from the two readers were averaged before statistical comparisons between the clinical and research scans.

Statistical Analysis

All continuous variables were tested using the Lilliefors test for normality and are presented as mean ± standard deviation (normal distribution) or median [25th percentile, 75th percentile] (non-normal distribution). Categorical variables are expressed as counts and percentages. Quantitative measurements derived from the clinical and research CE-MRA were compared using two-tailed paired student t-tests (normal distribution) or Wilcoxon signed-rank tests (non-normal distribution). Inter observer variability of the SI, CR, and thoracic aortic diameters were evaluated by calculating Intraclass Correlation Coefficients (ICC, two-way mixed, single measures, absolute agreement). An ICC > 0.9 was considered excellent agreement (21). Wilcoxon signed-rank tests were used to evaluate for qualitative differences in overall image quality, vessel wall conspicuity, and artifact scores between the standard of care and research scans. Inter observer variability for qualitative scores was calculated using weighted Cohen's kappa (κ) coefficient (poor agreement, κ = 0; slight agreement, κ = 0.01–0.20; fair agreement, κ = 0.21–0.40; moderate agreement, κ = 0.41–0.60; good agreement, κ = 0.61–0.80; and excellent agreement, κ = 0.81–1.00) (22). Bland-Altman analyses and Pearson correlation analyses were performed to compare the SI, CR, and aortic diameters derived from the two scans. All statistical analyses were conducted in SPSS (Version 23.0; IBM Corp). P-values less than 0.05 were considered statistically significant.

Results

All CE-MRA examinations were completed successfully, and all contrast agent administrations were performed without complications. None of the CE-MRA studies had poor image quality due to sub-optimal ECG-gating or poor breath-hold. Figure 2 presents representative images obtained from three different subjects using gadobutrol and gadoterate meglumine for contrast enhancement.

Quantitative Analysis

Gadobutrol demonstrated significantly higher SI at the MAAo, AArch, and DAo when compared to gadoterate meglumine (MAAo: gadobutrol 234 ± 97 vs. gadoterate meglumine 116 ± 29, $p < 0.001$; AArch: gadobutrol 206 ± 92 vs. gadoterate meglumine 99 ± 24, $p < 0.001$; DAo: gadobutrol 265 ± 132 vs. gadoterate meglumine 102 ± 28, $p < 0.001$). CR with respect to trapezius muscle did not show any significant difference between gadobutrol and gadoterate meglumine (MAAo: gadobutrol 3.0 ± 1.1 vs. gadoterate meglumine 2.7 ± 1.0, $p = 0.503$; AArch: gadobutrol 2.7 ± 1.0 vs. gadoterate meglumine 2.8 ± 1.1, $p = 0.599$; DAo: gadobutrol 3.3 ± 1.5 vs. gadoterate meglumine 3.0 ± 1.1, $p = 0.099$). The distribution of the SI and CR measurements are shown in detail in Fig. 3.

The vessel-lumen diameters derived from gadobutrol-enhanced MRA and gadoterate meglumine-enhanced MRA did not show significant differences at the sinus of Valsalva (gadobutrol: 4.2 ± 0.4 vs. gadoterate meglumine: 4.3 ± 0.4, $p = 0.571$), sinotubular junction (gadobutrol: 3.5 ± 0.5 vs. gadoterate meglumine: 3.5 ± 0.4, $p = 0.221$), MAAo (gadobutrol: 3.7 ± 0.6 vs. gadoterate meglumine: 3.7 ± 0.6, $p = 0.563$), proximal AArch (gadobutrol: 3.3 ± 0.5 vs. gadoterate meglumine: 3.2 ± 0.5, $p = 0.151$), distal AArch (gadobutrol: 2.6 ± 0.3 vs. gadoterate meglumine: 2.6 ± 0.3, $p = 0.088$), or distal DAo (gadobutrol: 2.4 ± 0.3 vs. gadoterate meglumine: 2.4 ± 0.3, $p = 0.821$). The distribution of the measurements is shown in detail in Fig. 4.

Figure 5A shows scatter plots from linear regression analysis illustrating weak correlation between the SI ($r = 0.18$), moderate correlation between the CR ($r = 0.40$), and strong correlations between the diameters ($r = 0.98$) derived from the two GBCAs. Figure 5B shows Bland-Altman plots illustrating poor agreement between the SI (mean difference = -130; the upper and lower limits of agreement = -130 ± 210), moderate agreement between the CR (mean difference = 0.02; the upper and lower limits of agreement = 0.02 ± 2.6), and good agreement between the diameters (mean difference = -0.2mm; the upper and lower limits of agreement = -0.2 ± 3.2mm).

Tables 2A and 2B shows the interobserver variability of the quantitative measurements derived from gadobutrol-enhanced MRA and gadoterate meglumine-enhanced MRA, respectively.

Table 2. Interobserver variability analysis of quantitative measurements

Gadobutrol	Reader 1	Reader 2	ICC
Signal Intensity			
Mid-ascending Aorta	229 ± 74	228 ± 71	1.00
Aortic Arch	203 ± 65	201 ± 64	1.00
Distal Descending Aorta	275 ± 118	276 ± 121	1.00
Contrast Ratio with respect to muscle			
Mid-ascending Aorta	3.3 ± 1.4	3.6 ± 1.6	0.98
Aortic Arch	2.9 ± 1.3	3.1 ± 1.4	0.98
Distal Descending Aorta	3.8 ± 1.8	3.3 ± 1.5	0.98
Luminal diameters			
Sinus of Vasalva	4.0 ± 0.4	4.1 ± 0.4	0.79
Sinotubular Junction	3.5 ± 0.6	3.5 ± 0.6	0.99
Mid-ascending Aorta	3.7 ± 0.7	3.8 ± 0.6	0.98
Proximal Arch	3.2 ± 0.6	3.2 ± 0.5	0.99
Distal Arch	2.6 ± 0.3	2.5 ± 0.3	0.95
Distal Descending Aorta	2.5 ± 0.3	2.4 ± 0.3	0.99

Gatoterate meglumine	Reader 1	Reader 2	ICC
Signal Intensity			
Mid-ascending Aorta	125 ± 32	121 ± 31	0.98
Aortic Arch	106 ± 26	115 ± 27	0.98
Distal Descending Aorta	112 ± 24	115 ± 24	0.99
Contrast Ratio with respect to muscle			
Mid-ascending Aorta	3.6 ± 1.5	3.3 ± 1.2	0.98
Aortic Arch	3.1 ± 1.3	3.1 ± 1.1	0.98
Distal Descending Aorta	3.3 ± 1.4	3.1 ± 1.0	0.98
Luminal diameters			
Sinus of Vasalva	4.1 ± 0.4	4.3 ± 0.4	0.82
Sinotubular Junction	3.5 ± 0.5	3.8 ± 0.6	0.96
Mid-ascending Aorta	3.7 ± 0.6	3.9 ± 0.6	0.95
Proximal Arch	3.1 ± 0.5	3.2 ± 0.6	0.98
Distal Arch	2.5 ± 0.3	2.6 ± 0.3	0.97
Distal Descending Aorta	2.5 ± 0.3	2.6 ± 0.4	0.95

Qualitative Analysis

As shown in Table 3 and Fig. 6, qualitative image grading revealed good to excellent overall image quality, wall conspicuity, and artifact scores for both gadobutrol and gadoterate meglumine-enhanced MRAs at the aortic root, MAAo, AArch, and DAo. In addition, we found no significant differences between the two GBCAs for the overall image quality, wall conspicuity, and artifact scores at any region.

Table 3
Comparison of qualitative scores between gadobutrol and gadoterate meglumine

	Gadobutrol	Gadoterate Meglumine	p-value
Overall Image Quality (1–5)			
Aortic Root	3.9 ± 0.8	3.8 ± 0.3	0.266
Mid-ascending Aorta	4.3 ± 0.6	4.2 ± 0.5	0.499
Aortic Arch	4.3 ± 0.7	4.2 ± 0.5	0.535
Distal Descending Aorta	4.5 ± 0.6	4.5 ± 0.5	0.622
Wall Conspicuity (0–4)			
Aortic Root	3.4 ± 0.5	3.3 ± 0.6	0.528
Mid-ascending Aorta	3.8 ± 0.3	3.8 ± 0.3	0.531
Aortic Arch	3.8 ± 0.4	3.8 ± 0.4	1.00
Distal Descending Aorta	3.8 ± 0.4	3.9 ± 0.2	0.909
Artifact (0–4)			
Aortic Root	3.1 ± 0.6	3.1 ± 0.6	0.937
Mid-ascending Aorta	3.7 ± 0.4	3.7 ± 0.4	0.771
Aortic Arch	3.6 ± 0.5	3.6 ± 0.5	0.909
Distal Descending Aorta	3.8 ± 0.3	3.9 ± 0.2	0.528

Table 4. Interobserver variability analysis of qualitative measurements

Gadobutrol	Reader 1	Reader 2	Cohen's Kappa
Overall Image Quality (1–5)			
Aortic Root	3.9 ± 0.9	4.0 ± 1.0	0.132
Mid-ascending Aorta	4.4 ± 0.7	4.2 ± 0.8	0.405
Aortic Arch	4.3 ± 0.8	4.2 ± 0.8	0.334
Distal Descending Aorta	4.5 ± 0.7	4.5 ± 0.6	0.385
Wall Conspicuity (0–4)			
Aortic Root	3.2 ± 0.8	3.5 ± 0.7	0.151
Mid-ascending Aorta	3.8 ± 0.4	3.8 ± 0.4	0.338
Aortic Arch	3.8 ± 0.4	3.7 ± 0.5	0.496
Distal Descending Aorta	3.8 ± 0.4	3.8 ± 0.4	0.496
Artifact (0–4)			
Aortic Root	3.2 ± 0.8	3.0 ± 0.7	0.117
Mid-ascending Aorta	3.8 ± 0.5	3.7 ± 0.5	0.325
Aortic Arch	3.8 ± 0.4	3.5 ± 0.7	0.427
Distal Descending Aorta	3.9 ± 0.4	3.8 ± 0.4	0.217

Gadoterate meglumine	Reader 1	Reader 2	Cohen's Kappa
Overall Image Quality (1–5)			
Aortic Root	3.6 ± 0.7	3.8 ± 0.8	0.217
Mid-ascending Aorta	4.2 ± 0.7	4.3 ± 0.6	0.263
Aortic Arch	4.1 ± 0.7	4.4 ± 0.6	0.124
Distal Descending Aorta	4.4 ± 0.6	4.5 ± 0.6	0.342
Wall Conspicuity (0–4)			
Aortic Root	3.2 ± 0.8	3.4 ± 0.8	0.151
Mid-ascending Aorta	3.9 ± 0.3	3.8 ± 0.5	-0.012
Aortic Arch	3.8 ± 0.5	3.8 ± 0.4	0.494
Distal Descending Aorta	3.9 ± 0.3	3.9 ± 0.3	0.203
Artifact (0–4)			
Aortic Root	3.2 ± 0.8	3.1 ± 0.7	0.219
Mid-ascending Aorta	3.7 ± 0.5	3.7 ± 0.5	0.349
Aortic Arch	3.7 ± 0.5	3.6 ± 0.6	0.413
Distal Descending Aorta	3.9 ± 0.3	3.9 ± 0.3	0.203

Discussion

The findings from our study demonstrate that: 1) gadobutrol has significantly higher SI than gadoterate meglumine at the MAAo, AArch, and DAo; 2) CRs with respect to the trapezius muscle between gadobutrol and gadoterate meglumine were not significantly different at the MAAo, AArch, and DAo; 3) the maximal intraluminal orthogonal diameter measurements were not significantly different at different planes measured; 4) evaluation of overall image quality, wall conspicuity, and artifacts did not show any significant difference between the two GBCAs at the aortic root, MAAo, AArch, or the DAo.

Previous studies have compared the performance of gadobutrol and gadoterate meglumine for CE-MRA demonstrating variable results at other body regions (13–20). Wuesten et al. found that, for low-dose, high temporal resolution CE-MRA of carotid artery aneurysms at 3T, gadobutrol was superior to gadoterate meglumine in terms of contrast-to-noise ratios (CNR) and depiction of morphological details (13). Similar observations were made by Morelli et al., who found that for renal artery stenosis assessment at 3T, low-dose gadobutrol (0.05 mmoL/kg) CE-MRA resulted in improved accuracy relative to equivalently dosed gadoterate meglumine (14). Kramer et al. found that, at equimolar doses, gadobutrol demonstrated higher signal-to-noise ratios (SNR), CNR, and superior image quality than

gadoterate meglumine for dynamic and static carotid CE-MRA at 3T (15). Hansmann et al. found that, for equimolar, low-dose, time-resolved CE-MRA protocol of the calves, the significantly better SNR and CNR provided by gadobutrol compared to gadoterate meglumine did not translate into substantial differences in image quality (16). Using digital subtraction angiography (DSA) as the reference standard, Loewe et al. found that gadoterate meglumine was not inferior to gadobutrol in terms of diagnostic performance in patients with peripheral arterial occlusive disease undergoing CE-MRA at equimolar dose at 3T (17). Haneder et al. found that, at equimolar doses, gadobutrol yielded significantly higher SNR and CNR while gadoterate was better rated in terms of overall image quality and diagnostic confidence for the evaluation of peripheral arterial occlusive disease (18). Hoelter et al. found that, gadobutrol resulted in a significantly higher SNR/CNR and better delineation of the intracranial vasculature when compared to gadoterate meglumine for cervical and cerebral CE-MRA at 1.5T (19). Lee et al. found that, at equimolar doses, increased gadolinium delivery over time using gadobutrol provides higher relative enhancement parameters in benign prostatic hyperplasia nodules compared with gadoterate meglumine but does not translate into improved SNR or CNR (20). However, results from CE-MRA studies of certain anatomical areas are not transferable to other areas without careful interrogation because the injection volume, injection rate, and the contrast agent travel time influence the concentration of GBCA in the region of interest significantly.

Due to their paramagnetic nature, GBCAs shorten the tissue relaxation time, resulting in increased tissue signal intensity on T1-weighted images (23). A higher relaxivity would amplify the T1 shortening effects, enabling CE-MRA to be performed at lower doses with a potential reduction of the risk of GBCA-induced toxicity. Previously, numerous studies in adult patients have shown that gadobutrol, due to its relatively higher r1 relaxivity (5.3 L $mmol^{-1}s^{-1}$ in blood at 37°C/1.5 T) (24), results in significantly improved image quality and diagnostic performance relative to that achieved with comparator GBCAs at equivalent dose. When compared to gadobutrol, gadoterate meglumine has a lower r1 relaxivity (4.2 L $mmol^{-1}s^{-1}$ in blood at 37°C/1.5 T) (24). The higher SI of gadobutrol when compared to gadoterate meglumine as demonstrated in the current study is likely due to these differences in relaxivities. This may also be more marked in the thoracic aorta as the contrast bolus is not significantly dispersed since it is close to the heart, unlike other more peripheral vascular regions, where the contrast bolus is more dispersed. However, the CR of the intravascular compartment with respect to the trapezius muscle showed no significant difference between the contrast agents in our study. This may reflect that part of the difference in the SI between the two exams maybe related to technical and/or patient-related differences as the two exams were done on separate days and separate machines. Another factor to consider for first-pass CE-MRA is edge blurring. Theoretically, edge blurring occurs if only the center parts of k-space are sampled during the presence of contrast agent in the region of interest and could be enhanced while using gadobutrol due to the smaller injected volume when compared to gadoterate meglumine. However, this was neither quantitatively measured nor reflected as impaired qualitative scores in our study. This suggests that 0.2 mmol/kg bodyweight of a 1.0 molar GBCA injected at 2.0 mL/sec has a sufficiently long contrast agent bolus to avoid disturbing edge blurring, i.e., contrast agent is present in the vascular territory of interest during the entire k-space sampling to an adequate degree.

In our study, a double dose of GBCAs was used for intraluminal contrast enhancement. This was because the standard-of-care clinical MRA was always performed in conjunction with a comprehensive cardiac MRI protocol. For research MRA, we matched the GBCA dose to the clinical MRA. Previous studies have demonstrated the safety (25) and superior signal-to-noise (26, 27) on higher dosing of GBCAs, but its effects on clinical practice may be negligible. Furthermore, in our study, we matched the flow rate of the two GBCA (2.0 mL/s). This may have led to a higher peak concentration of GB when compared to GM, influencing the SI measurements. Future studies matching the gadolinium injection rates have to be performed to evaluate the impact of flow rates on SI and image quality.

This study had some limitations. First, the size of our study population is relatively small. Prospective patient acquisition was difficult as they had to fulfill inclusion criteria as mentioned above. Second, we were not able to randomize patients to the order in which they received the two different GBCAs, as patient enrollment occurred after their standard-of-care gadobutrol-enhanced MRA. Our institution uses gadobutrol for clinical CE-MRA of the thoracic aorta. Third, although all the examinations were performed on 1.5-Tesla MR scanners, for some subjects, the clinical CE-MRA were performed on a different model (Avanto or Aera) than the research CE-MRA (always Aera).

In conclusion, this prospective intraindividual study comparing equal doses of gadobutrol and gadoterate meglumine demonstrates that for CE-MRA of the thoracic aorta, the CR with respect to muscle, aortic luminal diameter measurements, and qualitative assessment including overall image quality, vessel-wall conspicuity, and artifacts are comparable between the two GBCA. However, gadobutrol demonstrated a significantly higher aortic luminal SI when compared to gadobuterol meglumine. Future studies are warranted to evaluate the clinical impact of improved SI of gadobutrol for the assessment of the thoracic aorta.

Abbreviations

CE-MRA Contrast-Enhanced Magnetic Resonance Angiography

FP-MRA First-Pass Magnetic Resonance Angiography

GBCA Gadolinium-Based Contrast Agent

GRE Gradient Recalled Echo

GRAPPA GeneRalized Autocalibrating Partial Parallel Acquisition

bSSFP Balanced Steady-State Free-Precession

SI Signal Intensity

ROIs Regions of Interest

MAAo Mid-Ascending Aorta

AArch	Aortic Arch
DAo	Descending Aorta
CR	Contrast Ratios
STJ	Sinotubular Junction
ICC	Intraclass Correlation Coefficients
CNR	Contrast-to-Noise Ratios
SNR	Signal-to-Noise Ratios
DSA	Digital Subtraction Angiography

References

1. Krinsky G, Rofsky N, Flyer M, Giangola G, Maya M, DeCoroto D, Earls J, Weinreb J (1996) Gadolinium-enhanced three-dimensional MR angiography of acquired arch vessel disease. Am J Roentgenol 167(4):981–987
2. Godart F, Labrot G, Devos P, McFadden E, Rey C, Beregi JP (2002) Coarctation of the aorta: comparison of aortic dimensions between conventional MR imaging, 3D MR angiography, and conventional angiography. Eur Radiol 12(8):2034–2039
3. Di Cesare E, Giordano AV, Cerone G, De Remigis F, D'Eusanio G, Masciocchi C (2000) Comparative evaluation of TEE, conventional MRI and contrast-enhanced 3D breath-hold MRA in the post-operative follow-up of dissecting aneurysms. Int J Cardiac Imaging 16(3):135–147
4. Weigel S, Tombach B, Maintz D, Klotz S, Vestring T, Heindel W, Fischbach R (2003) Thoracic aortic stent graft: comparison of contrast-enhanced MR angiography and CT angiography in the follow-up: initial results. Eur Radiol 13(7):1628–1634
5. Garg SK, Mohan S, Kumar S (2011) Diagnostic value of 3D contrast-enhanced magnetic resonance angiography in Takayasu's arteritis—a comparative study with digital subtraction angiography. Eur Radiol 21(8):1658–1666
6. Krinsky GA, Rofsky NM, DeCorato DR, Weinreb JC, Earls JP, Flyer MA, Galloway AC, Colvin SB (1997) Thoracic aorta: comparison of gadolinium-enhanced three-dimensional MR angiography with conventional MR imaging. Radiology 202(1):183–193
7. Hiratzka LF, Bakris GL, Beckman JA, Bersin RM, Carr VF, Casey DE Jr, Eagle KA, Hermann LK, Isselbacher EM, Kazerooni EA, Kouchoukos NT, Lytle BW, Milewicz DM, Reich DL, Sen S, Shinn JA, Svensson LG, Williams DM, ACCF/AHA/AATS/ACR/ASA/SCA/SCAI (2010) /SIR/STS/SVM guidelines for the diagnosis and management of patients with Thoracic Aortic Disease: a report of the American College of Cardiology Foundation/American Heart Association Task Force on Practice

Guidelines, American Association for Thoracic Surgery, American College of Radiology, American Stroke Association, Society of Cardiovascular Anesthesiologists, Society for Cardiovascular Angiography and Interventions, Society of Interventional Radiology, Society of Thoracic Surgeons, and Society for Vascular Medicine. Circulation 2010;121(13):e266-369

8. Hadizadeh DR, Jost G, Pietsch H, Weibrecht M, Perkuhn M, Boschewitz JM, Keil VC, Träber F, Kukuk GM, Schild HH, Willinek WA (2014) Intraindividual quantitative and qualitative comparison of gadopentetate dimeglumine and gadobutrol in time-resolved contrast-enhanced 4-dimensional magnetic resonance angiography in minipigs. Invest Radiol 49(7):457–464
9. Lawaczeck R, Jost G, Pietsch H (2011) Pharmacokinetics of contrast media in humans: model with circulation, distribution, and renal excretion. Invest Radiol 46(9):576–585
10. Frenzel T, Lengsfeld P, Schirmer H, Hütter J, Weinmann HJ (2008) Stability of gadolinium-based magnetic resonance imaging contrast agents in human serum at 37 degrees C. Invest Radiol 43(12):817–828
11. Prince MR, Lee HG, Lee CH, Youn SW, Lee IH, Yoon W, Yang B, Wang H, Wang J, Shih TT, Huang GS, Lirng JF, Palkowitsch P (2017) Safety of gadobutrol in over 23,000 patients: the GARDIAN study, a global multicentre, prospective, non-interventional study. Eur Radiol 27(1):286–295
12. Szomolanyi P, Rohrer M, Frenzel T, Noebauer-Huhmann IM, Jost G, Endrikat J, Trattnig S, Pietsch H (2019) Comparison of the Relaxivities of Macrocyclic Gadolinium-Based Contrast Agents in Human Plasma at 1.5, 3, and 7 T, and Blood at 3 T. Invest Radiol 54(9):559–564
13. Wuesten O, Morelli JN, Miller MW, Tuzun E, Lenox MW, Fossum TW, Trelles M, Cotes C, Krombach GA, Runge VM (2012) MR angiography of carotid artery aneurysms in a porcine model at 3 tesla: Comparison of two different macrocyclic gadolinium chelates and of dynamic and conventional techniques. J Magn Reson Imaging 36(5):1203–1212
14. Morelli JN, Runge VM, Ai F, Zhang W, Li X, Schmitt P, McNeal G, Miller M, Lennox M, Wusten O, Schoenberg SO, Attenberger UI (2012) Magnetic Resonance Evaluation of Renal Artery Stenosis in a Swine Model: Performance of Low-Dose Gadobutrol Versus Gadoterate Meglumine in Comparison With Digital Subtraction Intra-Arterial Catheter Angiography. Invest Radiol 47(6):376–382
15. Kramer JH, Arnoldi E, François CJ, Wentland AL, Nikolaou K, Wintersperger BJ, Grist TM (2013) Dynamic and static magnetic resonance angiography of the supra-aortic vessels at 3.0 T: intraindividual comparison of gadobutrol, gadobenate dimeglumine, and gadoterate meglumine at equimolar dose. Invest Radiol 48(3):121–128
16. Hansmann J, Michaely HJ, Morelli JN, Luckscheiter A, Schoenberg SO, Attenberger UI (2014) Enhancement Characteristics and Impact on Image Quality of Two Gadolinium Chelates at Equimolar Doses for Time-Resolved 3-Tesla MR-Angiography of the Calf Station. PLoS ONE 9(6):e99079
17. Loewe C, Arnaiz J, Krause D, Marti-Bonmati L, Haneder S, Kramer U (2015) MR Angiography at 3 T of Peripheral Arterial Disease: A Randomized Prospective Comparison of Gadoterate Meglumine and Gadobutrol. Am J Roentgenol 204(6):1311–1321

18. Haneder S, Attenberger UI, Schoenberg SO, Loewe C, Arnaiz J, Michaely HJ (2012) Comparison of 0.5M gadoterate and 1.0M gadobutrol in peripheral MRA: A prospective, single-center, randomized, crossover, double-blind study. J Magn Reson Imaging 36(5):1213–1221
19. Hoelter P, Lang S, Weibart M, Schmidt M, Knott MFX, Engelhorn T, Essig M, Kloska S, Doerfler A (2017) Prospective intraindividual comparison of gadoterate and gadobutrol for cervical and intracranial contrast-enhanced magnetic resonance angiography. Neuroradiology 59(12):1233–1239
20. Lee CH, Vellayappan B, Taupitz M, Hamm B, Asbach P (2019) Dynamic contrast-enhanced MR imaging of the prostate: intraindividual comparison of gadoterate meglumine and gadobutrol. Eur Radiol 29(12):6982–6990
21. Koo TK, Li MY (2016) A Guideline of Selecting and Reporting Intraclass Correlation Coefficients for Reliability Research. J Chiropr Med 15(2):155–163
22. Cohen J (1968) Weighted kappa: nominal scale agreement with provision for scaled disagreement or partial credit. Psychol Bull 70(4):213–220
23. Shen Y, Goerner FL, Snyder C, Morelli JN, Hao D, Hu D, Li X, Runge VM (2015) T1 Relaxivities of Gadolinium-Based Magnetic Resonance Contrast Agents in Human Whole Blood at 1.5, 3, and 7 T. Invest Radiol 50(5):330–338
24. Rohrer M, Bauer H, Mintorovitch J, Requardt M, Weinmann H-J (2005) Comparison of Magnetic Properties of MRI Contrast Media Solutions at Different Magnetic Field Strengths. Invest Radiol 40(11):715–724
25. Thurnher SA, Capelastegui A, Del Olmo FH, Dondelinger RF, Gervás C, Jassoy AG, Keto P, Loewe C, Ludman CN, Marti-Bonmati L, Meusel M, da Cruz JP, Pruvo JP, Sanjuan VM, Vogl T (2001) Safety and effectiveness of single- versus triple-dose gadodiamide injection- enhanced MR angiography of the abdomen: a phase III double-blind multicenter study. Radiology 219(1):137–146
26. Jourdan C, Heverhagen JT, Knopp MV (2007) Dose comparison of single- vs. double-dose in contrast-enhanced magnetic resonance angiography of the carotid arteries: Intraindividual cross-over blinded trial using Gd-DTPA. J Magn Reson Imaging 25(3):557–563
27. Herborn CU, Runge VM, Watkins DM, Gendron JM, Naul LG (2008) MR angiography of the renal arteries: intraindividual comparison of double-dose contrast enhancement at 1.5 T with standard dose at 3 T. AJR Am J Roentgenol 190(1):173–177

Figures

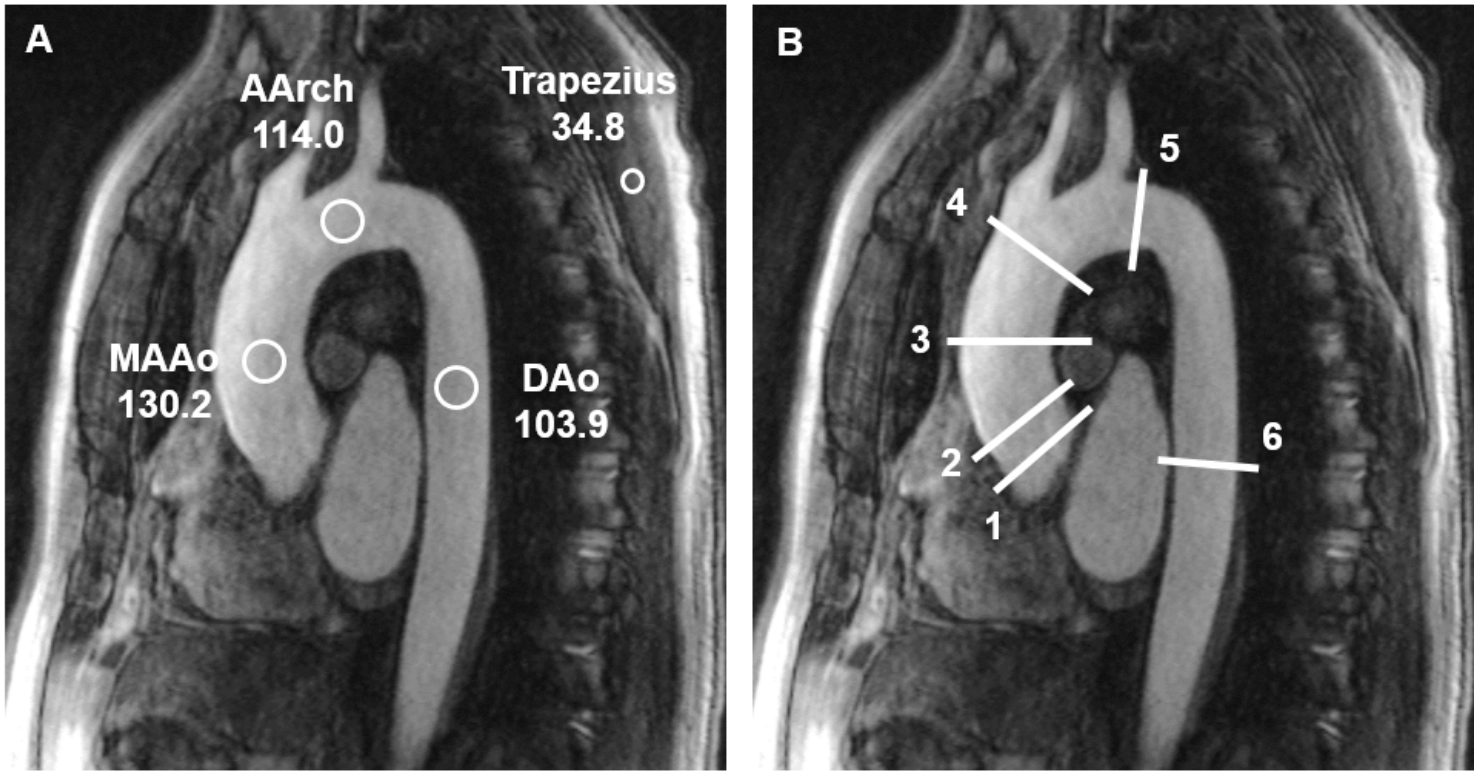

Figure 1

A. CE-MRA with ROIs drawn at the mid-ascending aorta (MAAo), aortic arch (AArch), descending aorta (DAo), and the trapezius muscle. B. CE-MRA with lines representing levels at which the luminal diameters were measured.

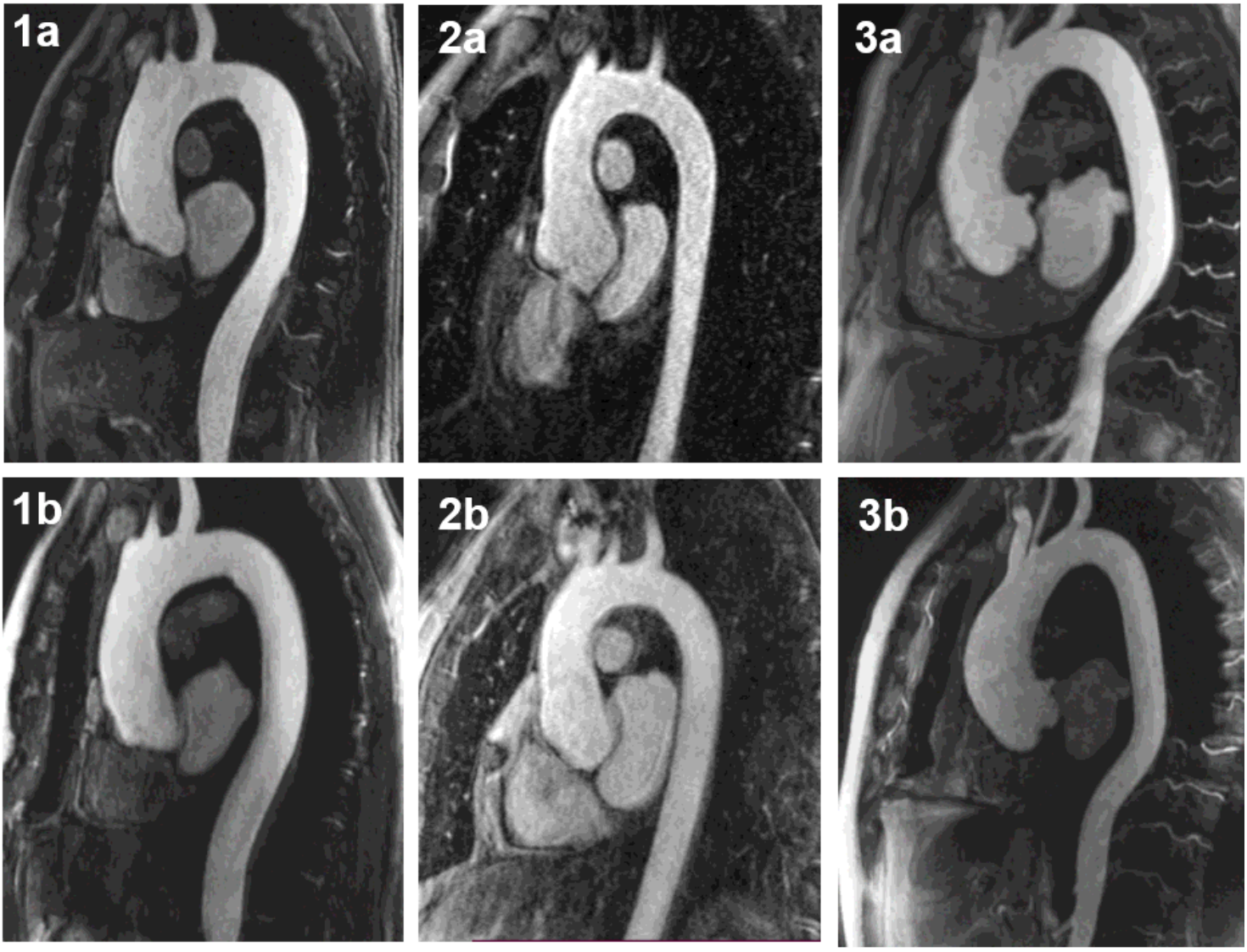

Figure 2

Representative thoracic aortic CE-MRA images of three different patients using gadobutrol (1a, 2a, 3a) and gadoterate meglumine (1b, 2b, 3b).

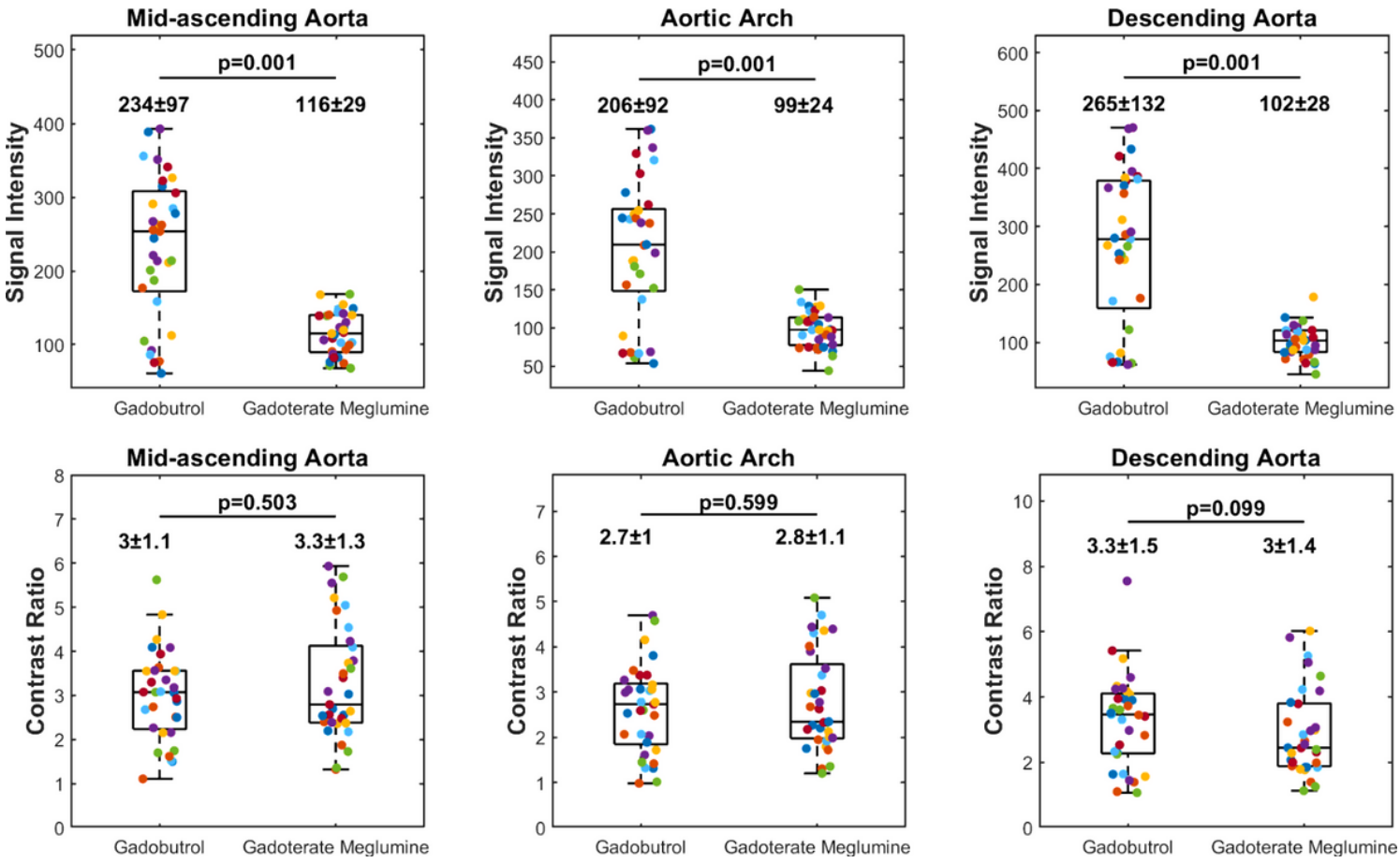

Figure 3

Comparison of the signal intensities and contrast ratios with respect to the muscle derived using gadobutrol and gadoterate meglumine. Each color represents measurements from one patient. Mean ± standard deviation and p-values are shown.

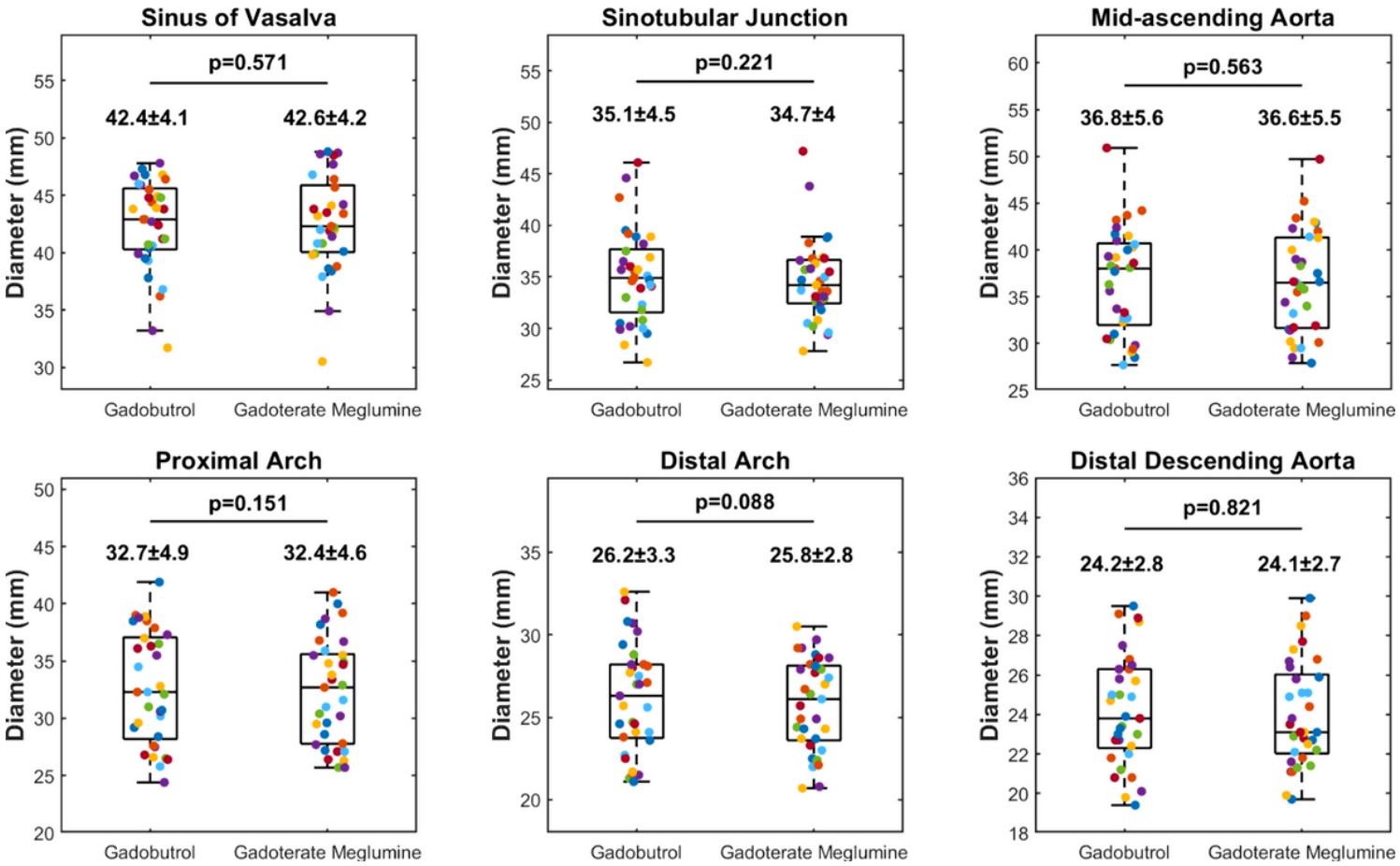

Figure 4

Comparison of the aortic diameters (in mm) derived using gadobutrol and gadoterate meglumine. Each color represents measurements from one patient. Mean ± standard deviation and p-values are shown.

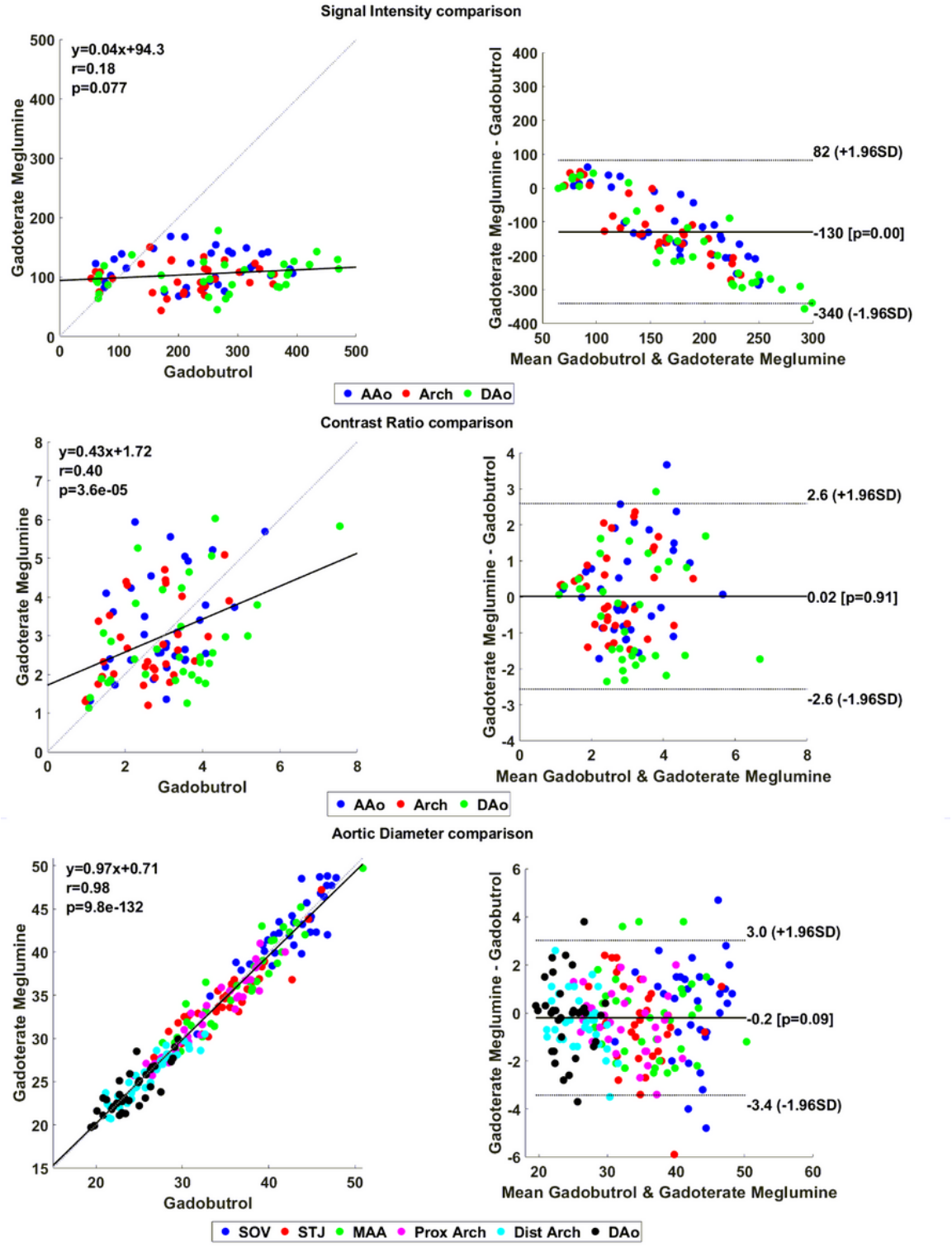

Figure 5

Linear regression and Bland-Altman plots comparing the Signal Intensity (panel A), Contrast Ratio (panel B), and aortic diameters (Panel C) derived from the gadobutrol-enhanced and gadoterate meglumine-enhanced MRAs.

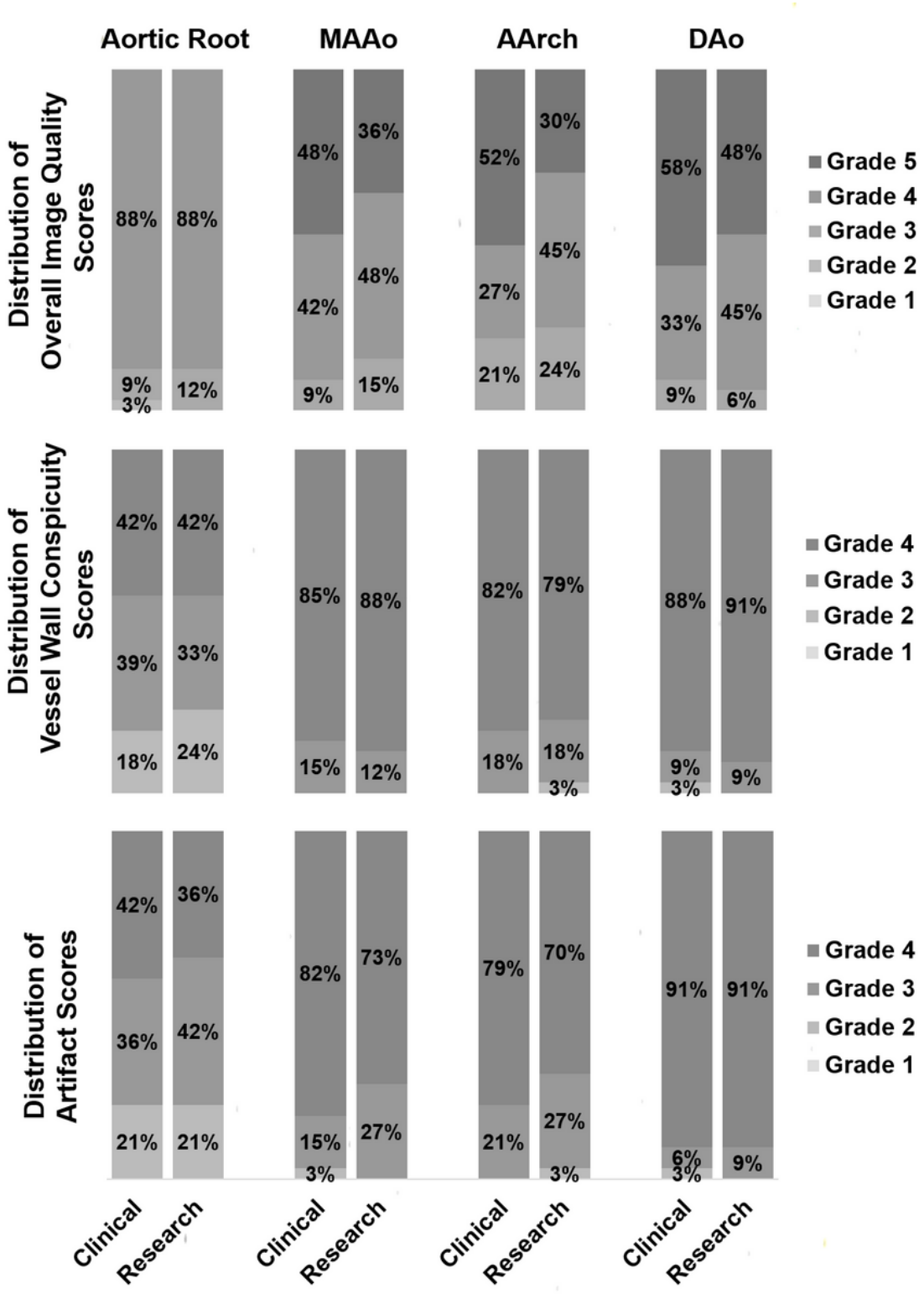

Figure 6

Diagrammatic representation of the distribution of qualitative scores from the two GBCAs.